Experimental Neurology 278 (2016) 105–115

Contents lists available at ScienceDirect

Experimental Neurology

journal homepage: www.elsevier.com/locate/yexnr

Reducing synuclein accumulation improves neuronal survival after spinal cord injury

Stephanie M. Fogerson [a,1], Alexandra J. van Brummen [a,b], David J. Busch [b,2], Scott R. Allen [a], Robin Roychaudhuri [c,3], Susan M.L. Banks [a], Frank-Gerrit Klärner [d], Thomas Schrader [d], Gal Bitan [c,e], Jennifer R. Morgan [a,*]

[a] Marine Biological Laboratory, The Eugene Bell Center for Regenerative Biology and Tissue Engineering, Woods Hole, MA 02543, United States
[b] Section of Molecular Cell and Developmental Biology, The University of Texas at Austin, Austin, TX 78712, United States
[c] Department of Neurology, David Geffen School of Medicine, University of California at Los Angeles, Los Angeles, CA 90095, United States
[d] Institute of Organic Chemistry, University of Duisburg-Essen, Essen 45117, Germany
[e] Brain Research Institute and Molecular Biology Institute, University of California at Los Angeles, Los Angeles, CA 90095, United States

ARTICLE INFO

Article history:
Received 28 December 2015
Received in revised form 29 January 2016
Accepted 4 February 2016
Available online xxxx

Keywords:
CLR01
Lamprey
Molecular tweezer
Neurodegeneration
Parkinson's disease
Synaptotagmin

ABSTRACT

Spinal cord injury causes neuronal death, limiting subsequent regeneration and recovery. Thus, there is a need to develop strategies for improving neuronal survival after injury. Relative to our understanding of axon regeneration, comparatively little is known about the mechanisms that promote the survival of damaged neurons. To address this, we took advantage of lamprey giant reticulospinal neurons whose large size permits detailed examination of post-injury molecular responses at the level of individual, identified cells. We report here that spinal cord injury caused a select subset of giant reticulospinal neurons to accumulate synuclein, a synaptic vesicle-associated protein best known for its atypical aggregation and causal role in neurodegeneration in Parkinson's and other diseases. Post-injury synuclein accumulation took the form of punctate aggregates throughout the somata and occurred selectively in dying neurons, but not in those that survived. In contrast, another synaptic vesicle protein, synaptotagmin, did not accumulate in response to injury. We further show that the post-injury synuclein accumulation was greatly attenuated after single dose application of either the "molecular tweezer" inhibitor, CLR01, or a translation-blocking synuclein morpholino. Consequently, reduction of synuclein accumulation not only improved neuronal survival, but also increased the number of axons in the spinal cord proximal and distal to the lesion. This study is the first to reveal that reducing synuclein accumulation is a novel strategy for improving neuronal survival after spinal cord injury.

1. Introduction

Spinal cord injury (SCI) damages neurons, leading to widespread neurodegeneration and neuronal death (Hains et al., 2003; Viscomi and Molinari, 2014). In mammals, loss of neurons, along with poor capacity for regeneration, contributes to the permanent impairment of movement and sensation after SCI (Blesch and Tuszynski, 2009). Though injury-induced neurodegeneration limits the extent of regeneration and spinal cord repair, very little is known about the mechanisms that cause injury-induced neurodegeneration or how to prevent it.

In a previous study, we reported a correlation between post-injury accumulation of synuclein and subsequent neuronal death (Busch and Morgan, 2012). Synucleins (α-, β-, γ-) comprise a family of synaptic vesicle-associated proteins whose physiological functions are still under investigation (Bendor et al., 2013). Under normal physiological conditions, α-synuclein regulates synaptic vesicle trafficking and protects nerve terminals from degeneration (Chandra et al., 2005; Nemani et al., 2010; Busch et al., 2014; Vargas et al., 2014; Wang et al., 2014). However, α-synuclein also has deleterious roles in Parkinson's disease (PD), dementia with Lewy bodies (DLB), multiple systems atrophy, and several variants of Alzheimer's disease, collectively called synucleinopathies. In these neurological diseases, α-synuclein abnormally self-assembles into oligomers and fibrils, leading to neurotoxicity and neuronal death (Lee and Trojanowski, 2006; Beyer and Ariza, 2008; Cookson, 2009). In familial Parkinson's disease, α-synuclein aggregation

Abbreviations: DLB, dementia with Lewy bodies; MO, morpholino; PD, Parkinson's disease; RS, reticulospinal; SCI, spinal cord injury; TBI, traumatic brain injury; ThT, thioflavin T.

* Corresponding author at: Marine Biological Laboratory, The Eugene Bell Center for Regenerative Biology and Tissue Engineering, 7 MBL St., Woods Hole, MA 02543, United States.
E-mail address: jmorgan@mbl.edu (J.R. Morgan).
[1] Department of Biology, Duke University, Durham, NC 27708, United States.
[2] Department of Biomedical Engineering, The University of Texas at Austin, Austin, TX 78712, United States.
[3] The Solomon H. Snyder Department of Neuroscience, Johns Hopkins School of Medicine, Baltimore, MD 21205, United States.

http://dx.doi.org/10.1016/j.expneurol.2016.02.004
0014-4886/

and neurotoxicity result from multiplication of the α-synuclein gene or from several point mutations (Cookson, 2009; Dawson et al., 2010). Thus, there are numerous links between α-synuclein aggregation and neurodegeneration in several common diseases. Though less well-studied, deposits of β- and γ-synuclein are associated with axon pathology in PD and DLB (Galvin et al., 1999), and overexpression of a DLB-linked β-synuclein mutant or wild type γ-synuclein causes neurodegeneration and behavioral defects in animal models (Ninkina et al., 2009; Fujita et al., 2010).

In comparison, very little is known about the roles for synuclein in the injured nervous system. There is growing evidence that both SCI and traumatic brain injury (TBI) lead to increased immunoreactivity against α-, β-, and γ-synucleins in mammals, including humans (Uryu et al., 2003; Uryu et al., 2007; Sakurai et al., 2009; Mondello et al., 2013). Furthermore, α-synuclein is elevated in the cerebral spinal fluid of patients with severe TBI, and higher α-synuclein levels have been associated with worse post-injury outcomes, including a greater extent of injury and even death (Su et al., 2011; Mondello et al., 2013). However, previous studies have not determined the effects of increased synuclein levels on the neurons themselves and have not examined the aggregation state of the protein. On one hand, increased amounts of synuclein may serve positive roles by protecting nerve terminals and supporting vesicle trafficking during membrane repair and axon regeneration (Bloom and Morgan, 2011). On the other hand, increased levels of synuclein may cause its aggregation and lead to neurotoxicity.

Our previous study was the first to reveal a correlation between injury-induced synuclein accumulation and dying neurons (Busch and Morgan, 2012). We used the large, identified reticulospinal (RS) neurons of lampreys because their injury responses can be followed over time on a cell-by-cell basis. RS neurons also express high levels of synuclein mRNA, which encodes for a γ-synuclein isoform. Using this model, we showed that a predictable and reproducible subset of giant RS neurons accumulated small puncta of synuclein protein after injury, and these were the same neurons that subsequently died. Conversely, the neurons that did not accumulate synuclein after SCI were the ones that survived the injury (Busch and Morgan, 2012), which is also the same subset that undergoes robust axon regeneration (Jacobs et al., 1997). After injury, the mRNA for γ-synuclein was downregulated in all of the giant RS neurons, implying post-transcriptional mechanisms (Busch and Morgan, 2012). We therefore concluded that synuclein accumulation is a biomarker for forthcoming neurodegeneration after SCI. However, the extent to which synuclein accumulation is causal for injury-induced neurodegeneration has not yet been assessed in any experimental model, forming the premise for the current study.

Here, we demonstrate that modulating post-injury synuclein accumulation using CLR01, a small-molecule inhibitor of amyloidogenic protein aggregation (Sinha et al., 2011), or a translation-blocking synuclein morpholino, leads to clearance of excess synuclein after SCI. Reducing post-injury synuclein accumulation improves the survival of injured neurons and increases the number of axons in the spinal cord. Thus, synuclein accumulation is identified here as a novel factor contributing to injury-induced neurodegeneration.

2. Materials and methods

2.1. Spinal cord transections and drug application

Late stage larval lampreys (*Petromyzon marinus*; 10–13 cm) were anesthetized in 0.1 g/L MS-222 (Tricaine-S; Western Chemical, Inc.; Ferndale, WA). Next, the spinal cord was transected at the 5th gill, as previously described (Busch and Morgan, 2012). CLR01 (2.4 μg = 1 mM) or buffer (lamprey internal solution: 180 mM KCl, 10 mM HEPES, pH 7.4) was added at the time and site of spinal injury *via* a small piece of Gelfoam (Pfizer; New York, NY). 3′-Lissamine labeled morpholinos (10 μg; GeneTools, LLC; Philomath, OR) were applied similarly. These included a translation-blocking synuclein morpholino (Syn MO) (5′CGCGTCCATTCCTCTTTCTTTGTCT3′) generated against the start site of lamprey γ-synuclein (GenBank Accession JN544525.1) and a five base pair mismatch synuclein morpholino (MM MO) that was used as the negative control (5′CGCcTgCATTgCTCTTTgTTTcTCT3′). Afterwards, lampreys were allowed to recover at room temperature (RT) for 11 weeks. Lampreys were then re-anesthetized, and the brains and spinal cords were dissected out for further experimentation by a researcher blinded to the experimental conditions. All procedures were approved by the Institutional Animal Care and Use Committees at The University of Texas at Austin and the Marine Biological Laboratory in accordance with standards set by the National Institutes of Health.

2.2. Immunofluoresence and image analysis

Brains and spinal cords were fixed overnight in 4% paraformaldehyde in 0.1 M PBS, pH 7.4. Immunofluoresence staining on whole mounted brains and cryosectioned spinal cords was done as previously described (Jin et al., 2009; Busch and Morgan, 2012). Briefly, the brains were labeled in whole mount with primary and secondary antibodies at 4 °C overnight, each followed by 5 × 1 h washes. Spinal cord sections were labeled with primary and secondary antibodies at RT for 1–2 h, each followed by 3 × 15 min washes. Primary antibodies used in this study included a rabbit polyclonal pan-synuclein antibody (1:100; Abcam ab6176; Cambridge, MA), a mouse monoclonal synaptotagmin 1 antibody (1:100; Developmental Studies Hybridoma Bank; DSHB mAb 48; Iowa City, IA), and a mouse monoclonal neurofilament-180 antibody (1:100; LCM16; kind gift from Dr. Michael Selzer), which have all been previously characterized in lamprey nervous tissues (Jin et al., 2009; Busch and Morgan, 2012; Lau et al., 2013). mAb 48 (asv 48) was deposited to the DSHB by L. Reichardt. For the pre-absorption experiment shown in Fig. 2D, the pan-synuclein antibody was incubated overnight at 4 °C with 100 μg/ml recombinant GST-tagged lamprey γ-synuclein before being applied to lamprey brains, and this resulted in a loss of the immunofluorescence signal. Secondary antibodies used in all experiments were AlexaFluor® 488-conjugated or AlexaFluor® 594-conjugated goat anti-rabbit or goat anti-mouse IgGs (1:300; Life Technologies; Grand Island, NY). Nuclei were stained with ProLong® Gold containing DAPI.

After immunostaining, the synuclein and synaptotagmin immunofluorescence in the cell bodies of giant RS neurons were imaged using a Zeiss LSM510 laser scanning confocal on an Axioskop 2FS upright microscope (10×, 0.3 NA Zeiss EC Plan-Neofluar objective or 40×, 0.8 NA Zeiss Achroplan water-dipping objective). Z-stacks were acquired, from which 3D projections were generated. For quantification of immunofluorescence, images were acquired under identical conditions for control and spinal-transected animals. Fluorescence intensity associated with each giant RS neuron was measured in ImageJ, followed by background subtraction using a measurement taken from the adjacent neuropil. Data from each cell type were collected and averaged from 6 to 13 lamprey brains.

NF-180 immunofluorescence and DAPI staining were imaged in spinal cord cryosections using an EVOS® FL Cell Imaging System (10×, 0.3 NA and 20×, 0.5 NA Plan-Fluorite objectives). Sections proximal, within, and distal to the lesion were sampled. For the axon analysis, all NF-180-labeled axons in the ventral half of the spinal cord were counted and averaged from 4 to 8 animals per condition.

2.3. Nissl staining and image analysis

After completing the immunofluorescence analysis, lamprey brains were Nissl-stained, as previously described (Busch and Morgan, 2012). Low-magnification images of lamprey brains were acquired either with a DFC420C camera connected to a Leica MZ10F stereoscope or an AxioCam MRc camera connected to a Zeiss SteREO Discovery V20. High-magnification images of individual M, I, and B cell regions were

acquired either with a Leica DMI 4000B microscope (HC PL Fluotar 10×/0.3 NA objective) or a SteREO Discovery V20 (PlanApo S 2.3× FWD 10 mm, 70× magnification). The mean intensity of the Nissl stain associated with each giant RS neuron was measured in ImageJ, followed by background subtraction using a measurement taken from the adjacent neuropil. Neurons that exhibited mean intensities greater than 0 were categorized as "Nissl (+)", and *vice versa*. All statistics and graphs were generated using Origin Pro 7.0.

2.4. Generation of recombinant lamprey γ-synuclein and aggregation analysis in vitro

GST-tagged lamprey γ-synuclein was purified from BL21 cells using a standard protocol. Then, the GST was cleaved off during a 16-h incubation at RT using thrombin (10 U/mg protein; GE Healthcare; Boston, MA). Untagged γ-synuclein was then separated from GST and thrombin using Glutathione Sepharose 4B beads and p-aminobenzamidine agarose (100 μl/50 U thrombin; A7155; Sigma; St. Louis, MO), respectively, and dialyzed into 0.1 M PBS, pH 7.4. Aggregation of the purified lamprey γ-synuclein was analyzed using a thioflavin T (ThT) fluorescence assay and confirmed by electron microscopy, as described previously (Roychaudhuri et al., 2014), except that 100 μM lamprey γ-synuclein was used with varying CLR01 concentrations.

3. Results

3.1. Spinal cord injury causes selective synuclein accumulation in poorly surviving neurons

To determine the extent to which post-injury synuclein accumulation causes neuronal death, we took advantage of the identified lamprey RS neurons due to their large size, as well as known capacities for degeneration and regeneration after SCI (Shifman et al., 2008; Busch and Morgan, 2012). There are 30 identified giant RS neurons in the lamprey midbrain and hindbrain, which are bilaterally positioned in stereotypical locations (Fig. 1). These are the mesencephalic cells (M cells: M1–M3), isthmic cells (I cells: I1–I5), bulbar Müller cells (B cells: B1–B6), and Mauthner neurons (Mth) (Rovainen, 1967). All giant RS neurons project their axons ipsilaterally into the spinal cord, except for the Mauthner neurons, which project contralaterally. Spinal cord transection thus severs the axons of all giant RS neurons (Fig. 1A). In the brains of uninjured, control lampreys, all of the giant RS neurons exhibit dark Nissl staining, indicating healthy neurons (Fig. 1B). However, after spinal transection, we and others have reported that a distinct and reproducible subset of the giant RS neurons degenerates, as demonstrated by swelling, loss of Nissl substance, and chromatolysis (Shifman et al., 2008; Busch and Morgan, 2012). The neurons that typically die after injury are M2, M3, I1, B1, B3, and Mth neurons (Fig. 1C, red arrows). These neurons also exhibit other signs of post-injury degeneration, including FluoroJadeC® staining (Busch and Morgan, 2012), TUNEL staining (Shifman et al., 2008), and increased levels of activated caspases (Barreiro-Iglesias and Shifman, 2012; Hu et al., 2013), suggesting a mechanism of apoptosis. In contrast, another subset of giant RS neurons typically survives (*e.g.* I3, I4, B2), as demonstrated by a retention of Nissl substance (Fig. 1C, black arrows). In keeping with terminology established in the literature, we refer to these classes of neurons as "poor survivors" and "good survivors," respectively (Fig. 1A) (Shifman et al., 2008; Busch and Morgan, 2012). The "good survivors" can be retrogradely labeled from a position caudal to the injury site, indicating that their axons readily regenerate (Jacobs et al., 1997; Shifman et al., 2008).

In our previous study, we showed that SCI induces an accumulation of synuclein only in the "poor survivors" (Busch and Morgan, 2012). Synuclein accumulation began as early as 1 week post-injury, when the neurons were still strongly Nissl stained, and increased further from 3 to 11 weeks post-injury when the neurons were chromalytic (Busch and Morgan, 2012). To corroborate and extend this finding, we examined the pre- and post-injury levels of synuclein and synaptotagmin, another synaptic vesicle-associated protein. We chose the 11 week post-injury time point because this is when maximal synuclein accumulation occurs (Busch and Morgan, 2012). Synuclein was immunolabeled in the lamprey brain using a pan-synuclein antibody raised against a highly conserved region of human α-synuclein (a.a. 11–26), which recognizes all lamprey and mammalian synucleins (Busch and Morgan, 2012). In the brains of uninjured, control lampreys, synuclein immunofluorescence levels were low, and the pattern of

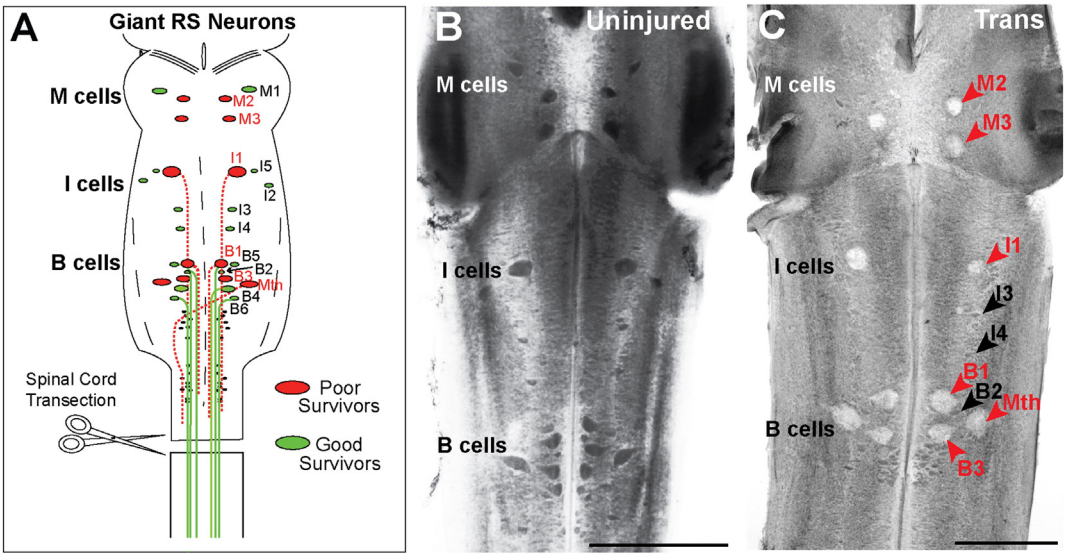

Fig. 1. A select subset of giant RS neurons dies after SCI. A. Diagram showing the 30 giant RS neurons in the lamprey brain and their stereotypical locations. These comprise the mesencephalic (M), isthmic (I), bulbar (B) and Mauthner (Mth) neurons. After spinal transection, which axotomizes all of the RS neurons, the subset of "poor survivors" (red) die, while "good survivors" (green) survive and regenerate their axons (Jacobs et al., 1997; Shifman et al., 2008). B–C. Bright field images of Nissl-stained lamprey brains showing the giant RS neurons. (B) In uninjured control lampreys all giant RS neurons are darkly stained, indicating healthy cells. (C) At 11 weeks post-transection (Trans), some of the giant RS neurons lose their Nissl stain, swell, and become chromalytic (red arrows), and these are typically the "poor survivors." In contrast, the "good survivors" retain strong Nissl stain (black arrows). Scale bars in B and C = 500 μm.

staining was diffuse within all of the giant RS neurons (Fig. 2A-B, E). In contrast, at 11 weeks post-injury, "poor survivor" neurons, such as M2, M3, I1, B3, and Mth, selectively accumulated synuclein throughout their somata (Fig. 2C, F), whereas the "good survivors" did not. The synuclein immunofluorescence signal was abolished after pre-absorption of the synuclein antibody with purified recombinant lamprey γ-synuclein, indicating specificity of the signal (Fig. 2D). High magnification imaging of giant RS neurons further revealed that the post-injury synuclein levels were higher, and the staining pattern was more punctate throughout the somata in the "poor survivors" (Fig. 2E-F). A quantitative analysis of the synuclein immunofluorescence intensity indicated that synuclein levels remained low in the "good survivors" after spinal cord injury (Fig. 2G) (Control: 5.3 ± 1.3 AU, n = 108 neurons, 6 brains; Transected: 9.3 ± 1.5 AU, n = 180 neurons, 10 brains; T-test; p = 0.07). In contrast, "poor survivors" exhibited a 4.5-fold increase in the overall synuclein immunofluorescence intensity (Fig. 2H) (Control: 10.2 ± 2.6 AU, n = 72 neurons, 6 brains; Transected: 45.5 ± 3.0 AU, n = 119 neurons, 10 brains; T-test; $p = 4.2 \times 10^{-14}$). Neurons that accumulated synuclein concomitantly exhibited signs of degeneration, including loss of Nissl substance (see Figs. 4C and 6C).

In contrast to synuclein, synaptotagmin levels did not significantly change after SCI (Fig. 2I–L). In a subset of the transected neurons, the synaptotagmin immunostaining pattern appeared slightly more punctate, though never to the degree observed with synuclein. The neuron shown in Fig. 2F and J, which was double-labeled for synuclein and synaptotagmin, demonstrates this observation. The overall synaptotagmin immunofluorescence intensity was not significantly changed after SCI in "good survivors" or "poor survivors" (Control — Good Survivors: 7.6 ± 1.5 AU, n = 108 neurons, 7 brains; Transected — Good Survivors: 5.0 ± 1.5 AU, n = 114 neurons, 7 brains; T-test; p = 0.23; Control — Poor Survivors: 14.9 ± 1.7 AU, n = 77 neurons, 7 brains; Transected — Poor Survivors: 21.0 ± 3.2 AU, n = 78 neurons, 7 brains; T-test; p = 0.09). Taken together, these results indicate that post-injury

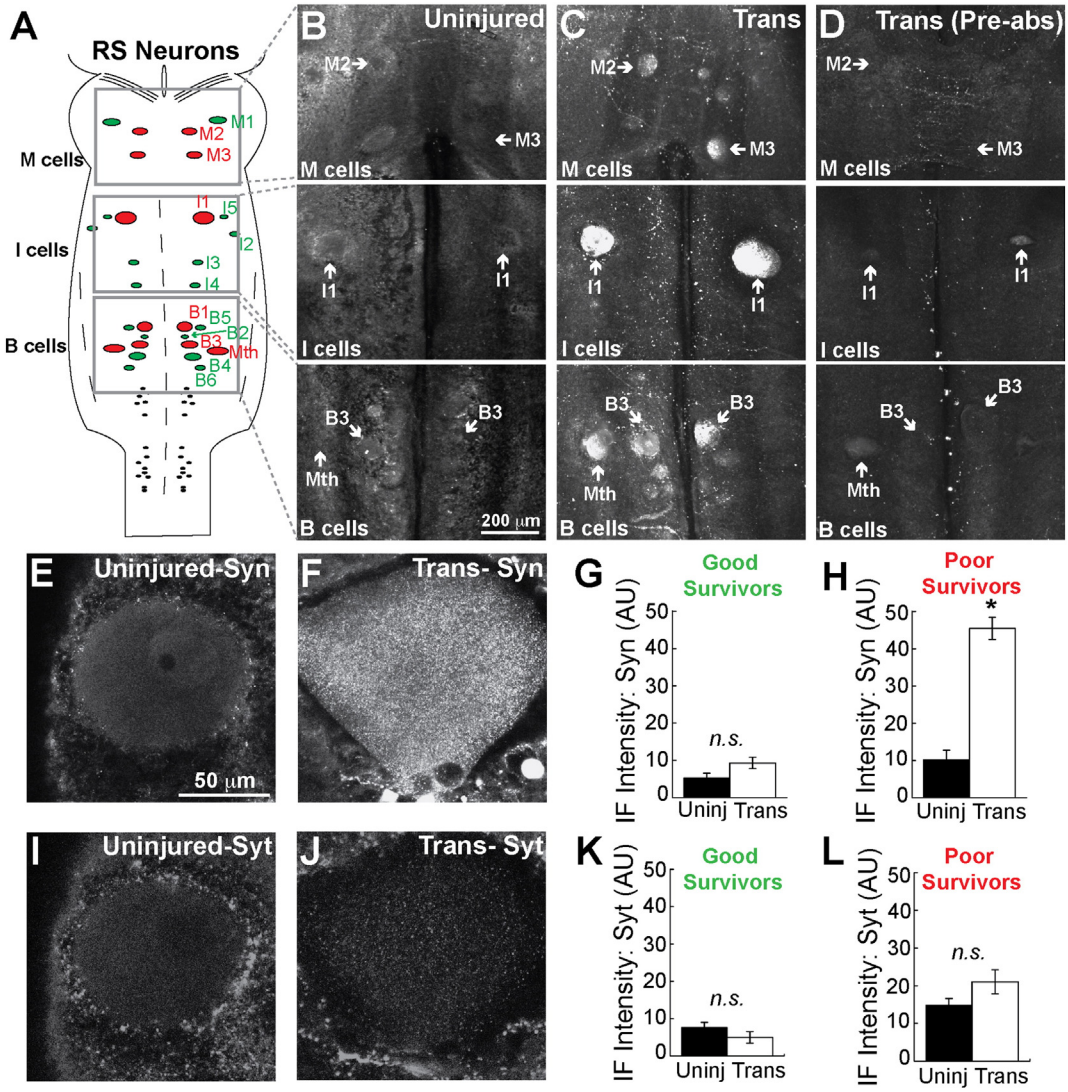

Fig. 2. Synuclein selectively accumulates in the "poor survivors" after spinal cord injury. A. Diagram of a lamprey brain showing the "poor survivors" (red) and "good survivors" (green), for reference. Boxes indicate the brain regions shown in B–D. B. Confocal projections showing synuclein immunofluorescence within the brain of an uninjured, control animal. Synuclein levels are low in all of the giant RS neurons. Arrows mark the positions of several giant RS neurons. C. In contrast, by 11 weeks post-transection (Trans), synuclein accumulated in the "poor survivors," such as M2, M3, I1, B3, and Mth. D. Pre-absorption of the synuclein antibody with recombinant synuclein abolished the post-injury immunofluorescence signal. Scale bar in B applies to C–D. E. Confocal image of an RS neuron at higher magnification. Synuclein (Syn) levels are low and diffuse in this uninjured I1 neuron. F. In contrast, after spinal transection, synuclein levels accumulated and became punctate in this B3 neuron. Scale bar in E applies to F, I, and J. G–H. Synuclein immunofluorescence (IF) intensity significantly increased only in the "poor survivors" after spinal transection. Bars represent mean ± S.E.M. from n = 72–180 neurons, 6–10 brains (T-test; *$p < 0.05$). I–J. Confocal images of the same neurons in E and F showing the immunofluorescence signal for synaptotagmin (Syt), another synaptic vesicle-associated protein. Synaptotagmin did not accumulate after transection. K–L. Synaptotagmin levels were not significantly altered after injury. Bars represent mean ± S.E.M. from n = 77–114 neurons, 7 brains (T-test; *n.s.* = not significant; $p > 0.05$).

synuclein accumulation is selective and occurs specifically within the "poor survivors," suggesting the possibility that it may play a role in injury-induced neurodegeneration.

3.2. CLR01 attenuates post-injury synuclein accumulation

As a first test to determine whether synuclein accumulation causes injury-induced neuronal death, we utilized the "molecular tweezer" inhibitor, CLR01 (Fig. 3A), a broad spectrum inhibitor of assembly and toxicity of amyloidogenic proteins, including α-synuclein, tau, and Aβ (Sinha et al., 2011). CLR01 remodels α-synuclein self-assembly and dissociates pre-formed α-synuclein fibrils (Sinha et al., 2011; Prabhudesai et al., 2012). It binds α-synuclein with sub-micromolar affinity with a primary binding site at the N-terminal Lys10/12 (Acharya et al., 2014). In cell culture models, CLR01 was shown to protect neurons from the toxicity of both exogenously added and endogenously expressed α-synuclein (Prabhudesai et al., 2012). CLR01 also reduces neurodegeneration and improves survival *in vivo* in a zebrafish model of α-synuclein neurotoxicity (Prabhudesai et al., 2012). It has also been shown to inhibit the aggregation of zebrafish γ-synuclein (Lulla, et al., 2016).

We initially tested whether CLR01 inhibited self-assembly of lamprey γ-synuclein (GenBank Accession JN544525.1), the synuclein isoform that is most highly expressed in the giant RS neurons (Busch and Morgan, 2012). Full-length lamprey γ-synuclein shares 56% amino acid identity and 83% similarity with human α-synuclein (Busch et al., 2014). Similar to human α-synuclein, recombinant lamprey γ-synuclein self-assembled into β-sheet-rich aggregates over time, as shown by an increase in thioflavin T (ThT) fluorescence (Fig. 3B). This *in vitro* synuclein aggregation was inhibited by CLR01 in a dose-dependent manner (Fig. 3B).

Next, a single dose of CLR01 (1 mM) or vehicle (buffer) was applied to the spinal cord at the time and site of transection *via* a small piece of Gelfoam, which is a standard approach for reagent delivery in other vertebrate SCI models, including fish (Becker et al., 2004; Williams et al., 2015). We estimate that reagents applied to the transection site are diluted 10–1000 times as they diffuse out of the Gelfoam, and so the effective concentration in the spinal cord is likely to be 1–100 μM, a range that is consistent with CLR01 effects in cell culture and zebrafish models of α-synuclein toxicity (Prabhudesai et al., 2012). At eleven weeks post-transection, in the vehicle-treated controls, synuclein accumulated into punctae in the "poor survivors", as expected (Fig. 3C, E). However, after CLR01 treatment, synuclein accumulation was greatly reduced within the giant RS neurons, and the staining pattern was more diffuse (Fig. 3D, F). Synuclein immunofluorescence intensity was statistically unchanged in "good survivors" after CLR01 treatment, likely because initial levels of synuclein were already low (Fig. 3G) (Con: 5.0 ± 1.1 AU, n = 232 neurons, 13 brains; CLR01: 5.6 ± 1.3 AU, n = 234 neurons, 13 brains; T-test; p = 0.7). In contrast, CLR01 significantly reduced synuclein immunofluorescence intensity by 34% in the "poor survivors" (Fig. 3G) (Con: 38.8 ± 3.4 AU, n = 154 neurons, 13 brains; CLR01: 25.7 ± 3.1 AU, n = 156 neurons, 13 brains; T-

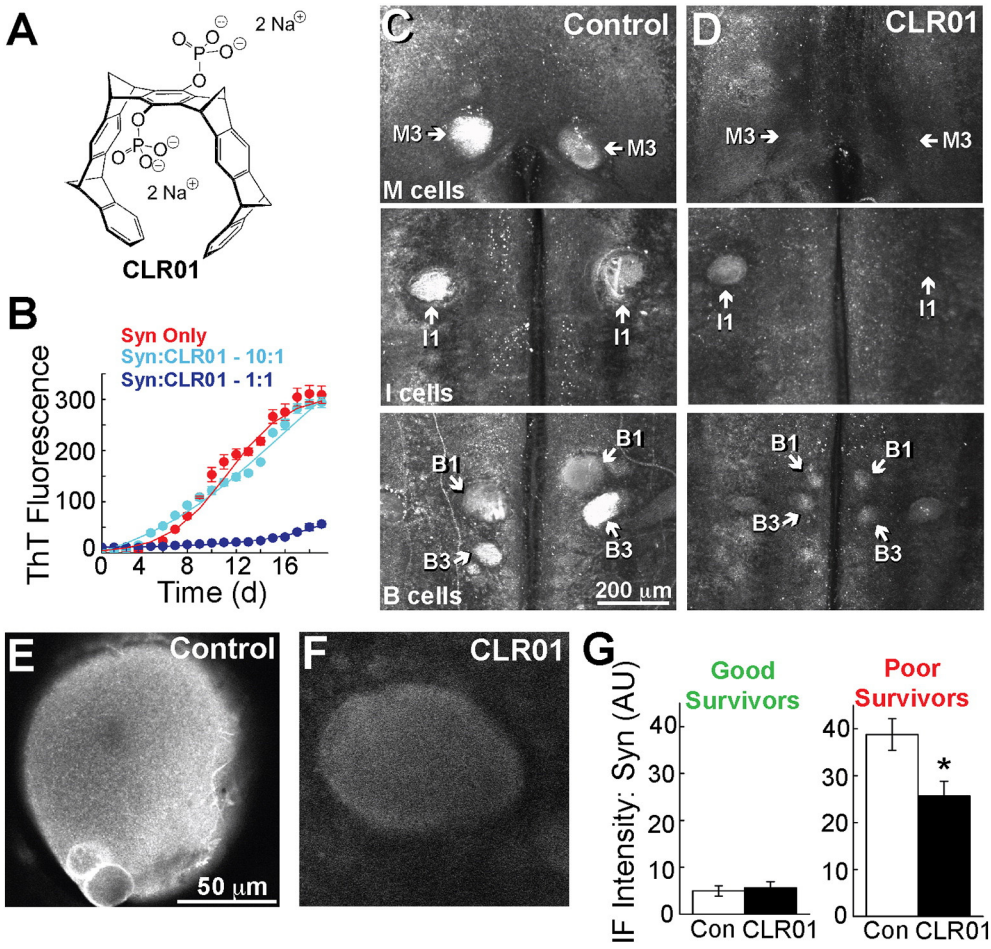

Fig. 3. CLR01 inhibits post-injury synuclein accumulation in RS neurons. A. Structure of CLR01. B. CLR01 inhibits the aggregation of lamprey γ-synuclein *in vitro*, as measured by a dose-dependent decrease in thioflavin T (ThT) fluorescence. Data points represent the mean ± SEM from n = 3 measurements. C–D. Confocal projections show that post-injury synuclein accumulation is greatly reduced in the RS neurons after CLR01 treatment. All images were taken at 11 weeks post-transection. Scale bar in C applies to D. E–F. Confocal images at higher magnification show that CLR01-treated neurons exhibited little to no synuclein accumulation. These are I1 neurons. Scale bar in E applies to F. G. CLR01 significantly reduced synuclein accumulation in the "poor survivors". Bars represent mean ± S.E.M. from n = 154–234 neurons, 13 brains (T-test; *p < *0.05*).

test; $p = 0.005$). Thus, application of CLR01 is an effective strategy for reducing post-injury synuclein accumulation in neurons.

3.3. CLR01 increases neuronal survival after SCI

Next, we used Nissl staining to assess the extent of neuronal survival after CLR01 treatment in order to determine whether synuclein accumulation plays a role in injury-induced neurodegeneration. As described above, a dark, uniform Nissl stain marks healthy RS neurons, whereas degenerating RS neurons have little or no Nissl substance and appear swollen and chromalytic. Eleven weeks after spinal transection, the brains of vehicle-treated animals exhibited many degenerating neurons, and the vast majority were "poor survivors" such as M2, M3, I1, B1, B3, and Mth neurons (Fig. 4A; red arrows). The neurons that lost Nissl staining also exhibited synuclein accumulation, as previously reported (Fig. 4C) (Busch and Morgan, 2012). In contrast, CLR01 reduced the number of degenerating neurons (Fig. 4B, D; red arrows) and increased the number of neurons that retained strong Nissl staining (Fig. 4B, D, white arrows), indicating greater neuronal survival. We subsequently performed a cell-by-cell analysis on the giant RS neurons from the brains of vehicle- and CLR01-treated animals ($n = 26$ neurons/cell type, 13 brains for each condition). Most individual giant RS neurons, including all the "poor survivors," exhibited an increase in post-injury survival after CLR01, as determined by an increase in the percentage of neurons that remained Nissl stained (Fig. 4E). Supporting the compound's safety, CLR01 did not negatively affect the "good survivor" population at 11 weeks post-transection (Fig. 4F) (Good Survivors – Con: 93.2 ± 1.4%, $n = 232$ neurons, 13 brains; CLR01: 95.7 ± 1.1%, $n = 234$ neurons, 13 brains; T-test, $p = 0.2$). Notably, however, CLR01 caused a significant 4.6-fold increase in the percentage of Nissl stained "poor survivors" (Fig. 4F) (Poor Survivors – Con: 7.9 ± 2.7%, $n = 154$ neurons, 13 brains; CLR01: 36.5 ± 6.6%, $n = 156$ neurons, 13 brains; T-test, $p = 5.1 \times 10^{-4}$). Thus, CLR01 reduced the accumulation of synuclein and improved neuronal survival after SCI.

3.4. Targeted knockdown of synuclein attenuates post-injury synuclein accumulation

As a second test to assess synuclein's role in injury-induced neurodegeneration, we inhibited synuclein protein production using a translation-blocking synuclein morpholino (Syn MO). As a control, we used a 5-base pair mismatch synuclein morpholino (MM MO). The lissamine-labeled morpholinos were loaded at the time and site of spinal transection, as is standard in zebrafish and lamprey SCI models (Becker et al., 2004; Zhang et al., 2015). Afterwards, fluorescence in the cell body indicated that the morpholinos were retrogradely transported to the RS neuron cell bodies, where they remained up to 11 weeks post-transection (Fig. 5A). Synuclein accumulation still occurred in the "poor survivors" in lampreys treated with the control mismatch MO (Fig. 5B, white arrows). We also observed some atypical synuclein accumulation in a subset of the "good survivors," such as B4 (Fig. 5B, yellow arrow), I3 and B2. In contrast, synuclein accumulation was substantially reduced after treatment with the Syn MO (Fig. 5C). As with CLR01, Syn MO treatment reduced the post-injury synuclein immunofluorescence signal, which was also less punctate and more diffuse (Fig. 5D–E). Quantitatively, Syn MO significantly reduced synuclein immunofluorescence in both "good survivors" and "poor survivors", when compared to the control mismatch MO (Fig. 5F) (Good Survivors – MM MO: 26.0 ± 2.4 AU, $n = 108$ neurons, 6 brains; Syn MO: 17.7 ± 1.4 AU, $n = 140$ neurons, 8 brains; T-test; $p = 0.002$; Poor Survivors – MM MO: 40.7 ± 3.7 AU, $n = 72$ neurons, 6 brains; Syn MO: 26.5 ± 2.5 AU, $n = 96$ neurons, 8 brains; T-test; $p = 0.001$). Thus, treatment with a translation-blocking synuclein morpholino is another effective strategy for reducing post-injury synuclein accumulation in neurons.

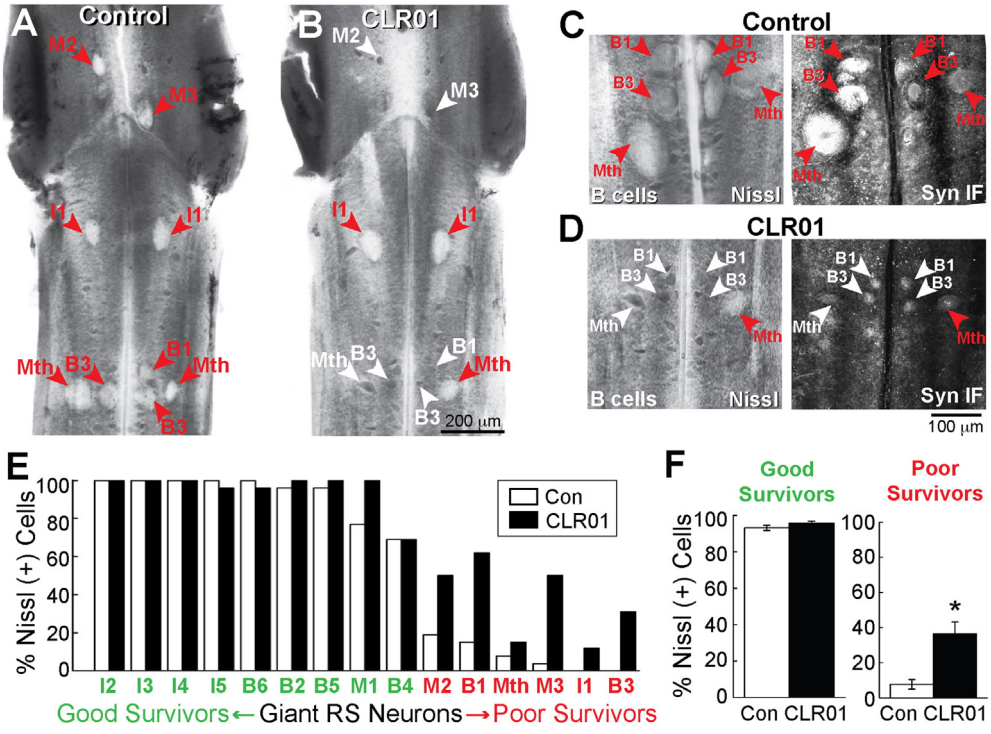

Fig. 4. CLR01 treatment improves neuronal survival after SCI. A–B. Nissl-stained lamprey brains at 11 weeks post-transection after treatment with vehicle (Control) or CLR01. After CLR01, there were fewer degenerating RS neurons (red arrows) and a greater number of surviving neurons (white arrows). Scale bar in B applies to A. C. Higher magnification images show Nissl staining (left) and synuclein immunofluorescence (Syn IF: right) on the B cell region from the same brain. In the absence of CLR01, there were many degenerating neurons that concomitantly accumulated synuclein (red arrows). D. In contrast, after CLR01 treatment, there were fewer degenerating neurons (red arrows) and a greater number of healthy neurons (white arrows), and synuclein accumulation was reduced. Scale bar in D applies to C. E. CLR01 improved the survival of most individual RS neurons. F. At the population level, CLR01 significantly improved survival of the "poor survivors". Bars represent mean ± S.E.M. from $n = 13$ brains (T-test; *$p < 0.05$).

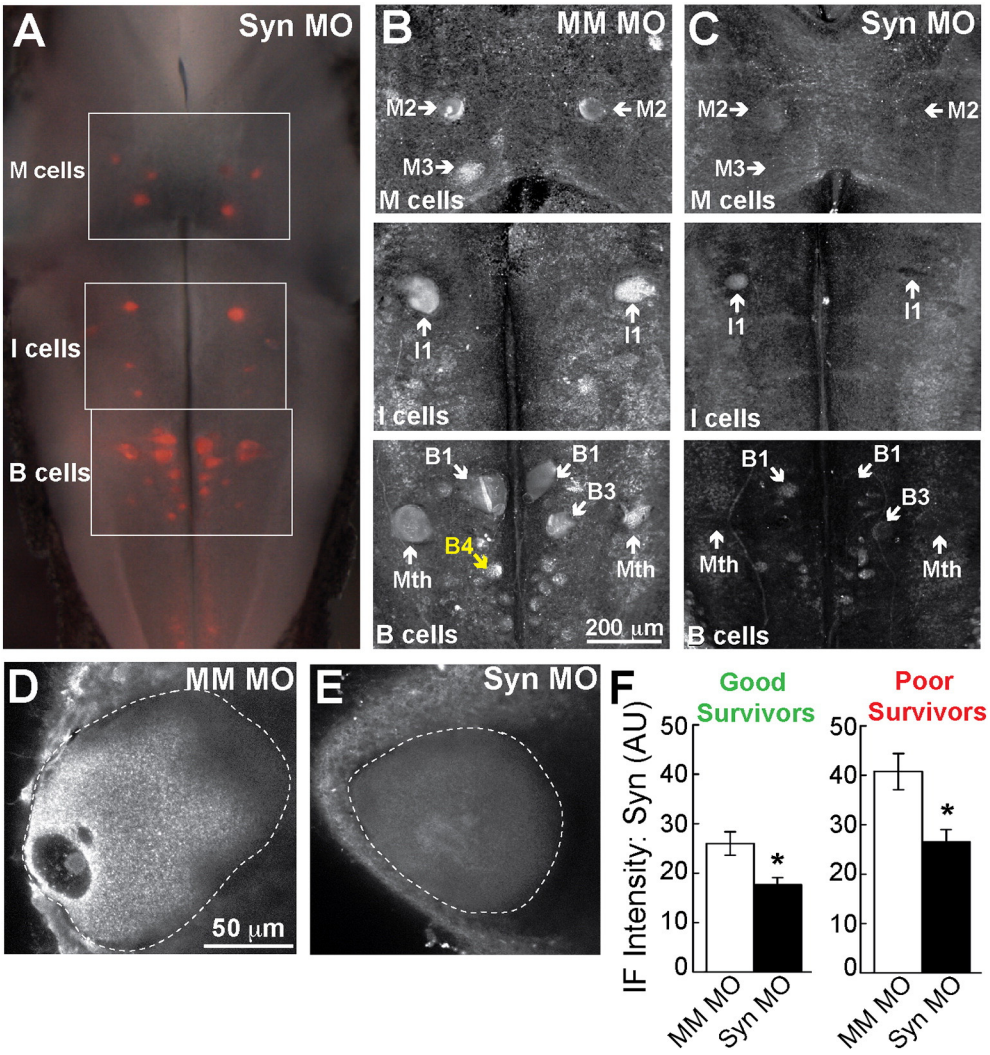

Fig. 5. Knockdown of post-injury synuclein accumulation with a translation-blocking morpholino. A. Bright field image of a lamprey brain, overlaid with a fluorescence image showing the RS neurons that were backfilled with a lissamine-conjugated synuclein morpholino (Syn MO; red). B–C. Confocal projections show that, compared to treatment with the 5-base pair mismatch morpholino (MM MO), post-injury synuclein accumulation is greatly reduced after treatment with the synuclein MO (Syn MO). In these experiments, the MM MO caused slightly elevated synuclein accumulation in some "good survivors" such as B4 (yellow arrow). All images were taken at 11 weeks post-transection. Scale bar in B applies to C. D–E. Confocal images at higher magnification show that Syn MO-treated neurons exhibited much less synuclein accumulation. Scale bar in D applies to E. Dotted lines indicate the borders of the RS neurons. F. Syn MO significantly reduced synuclein levels in both "good survivors" and "poor survivors". Bars represent mean ± S.E.M. from n = 72–140 neurons, 6–8 brains (T-test; *p < *0.05*).

3.5. Knockdown of synuclein increases neuronal survival and axon plasticity after SCI

Similar to CLR01, synuclein knockdown decreased the number of degenerating neurons and increased the number of surviving neurons at 11 weeks after spinal transection (Fig. 6A–D). Increased neuronal survival was observed for all of the "poor survivors" after synuclein knockdown (Fig. 6E). We also observed that Syn MO also improved the survival of most "good survivors" (Fig. 6E), likely because the control mismatch MO caused greater synuclein accumulation (Fig. 5F) and fewer Nissl stained "good survivors" (Fig. 6F) than is typically observed (compare with Fig. 4E–F) (see also Lau et al., 2013). Indeed, a quantitative analysis revealed that Syn MO significantly increased the percentage of Nissl stained "good survivors," indicating greater neuronal survival (Fig. 6F) (MM MO: 80.2 ± 5.4%, n = 108 neurons, 6 brains; Syn MO: 95.7 ± 1.4%, n = 140 neurons, 8 brains; T-test; p = 0.008). Syn MO also significantly increased the survival of "poor survivors" nearly 2-fold (Fig. 6F) (MM MO: 27.8 ± 8.2%, n = 72 neurons, 6 brains; Syn MO: 47.3 ± 4.8%, n = 96 neurons, 8 brains; T-test; p = 0.05). Across the entire population of thirty giant RS neurons, knockdown of post-injury synuclein accumulation significantly improved neuronal survival by ~20% (MM MO: 58.1 ± 6.6%, n = 180 neurons, 6 brains; Syn MO: 76.5 ± 1.7%, n = 236 neurons, 8 brains; T-test; p = 0.009). Thus, selectively reducing synuclein accumulation, by decreasing its production, is another effective strategy for sparing neurons after SCI.

Since synuclein knockdown improved post-injury neuronal survival, a natural prediction is that this may lead to a greater number of axons in the spinal cord. To test this, we labeled and counted the number of large axons in the ventral spinal cord where the giant RS axons are located. In uninjured lamprey spinal cords, most giant RS axons are clustered within the ventromedial tract, except for the Mauthner axons, which are positioned more laterally (Fig. 7A). An antibody raised against lamprey neurofilament-180 (NF-180) reliably labeled all thirty giant RS axons in the ventral spinal cord (30.4 ± 3.6 axons; n = 5 spinal cords), as well as some medium caliber sensory axons in the dorsal spinal cord (Fig 7B). We next used the NF-180 antibody to label spinal axons after injury. At 11 weeks post-transection, spinal cords treated with the control mismatch MO exhibited fewer NF-180 labeled axons

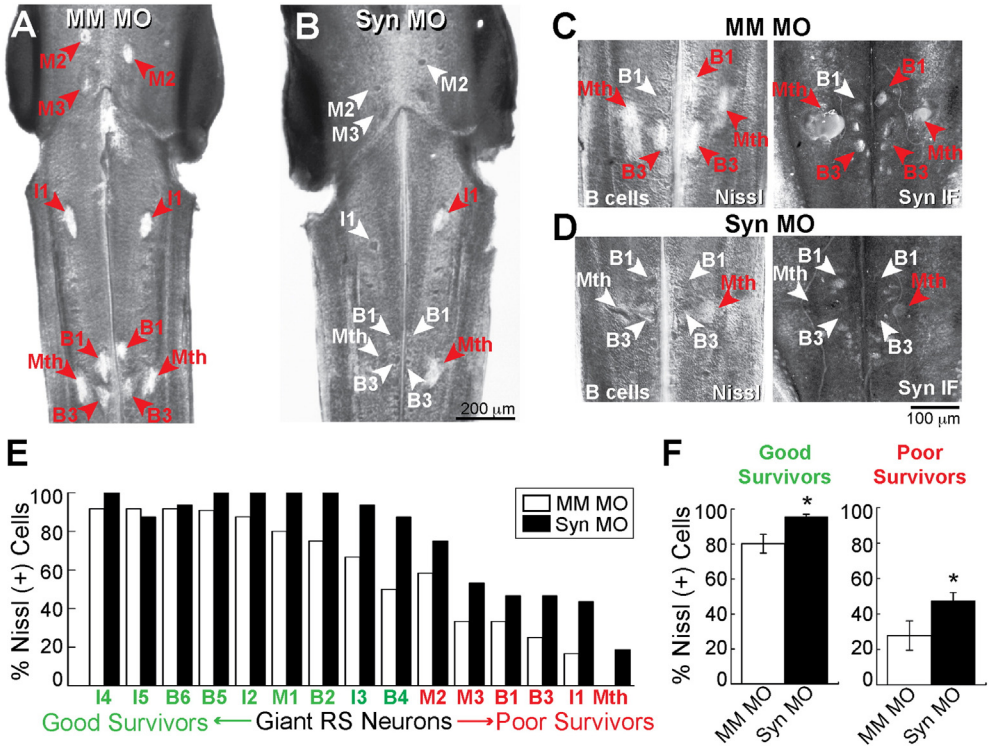

Fig. 6. Synuclein knockdown improves neuronal survival after SCI. A–B. Nissl-stained lamprey brains at 11 weeks post-transection after treatment with a control morpholino (MM MO) or the synuclein morpholino (Syn MO). After Syn MO, there were fewer degenerating RS neurons (red arrows) and a greater number of surviving neurons (white arrows). Scale bar in B applies to A. C. Higher magnification images show Nissl staining (left) and synuclein immunofluorescence (Syn IF: right) on the B cell region from the same brain. With MM MO, there were many degenerating neurons that also accumulated synuclein (red arrows). D. In contrast, after Syn MO, there were fewer degenerating neurons (red arrows) and a greater number of healthy neurons (white arrows). Scale bar in D applies to C. E. Syn MO improved the survival of most individual RS neurons. F. At the population level, Syn MO significantly improved survival of both "good survivors" and "poor survivors". Bars represent mean ± S.E.M. from n = 6–8 brains (T-test; *$p < 0.05$).

at locations 1456 μm proximal (Fig. 7C) and 488 μm distal (Fig. 7D) to the lesion site, and these axons were generally smaller than those in uninjured spinal cords. In the distal spinal cord, in particular, the axons tended to be located more laterally (Fig. 7D), as has been demonstrated previously for regenerated RS axons (Yin and Selzer, 1983; Oliphint et al., 2010). We quantified the number of NF-180 labeled axons in the ventral spinal cord (Fig. 7G), where the giant RS axons reside, at five separate locations with respect to the center of the lesion: proximal (−1456 and −784 μm), within (0 μm), and distal (+112 and +488 μm). This analysis revealed that spinal cords treated with the control MM morpholino exhibited similar numbers of axons to untreated, transected spinal cords at 11 weeks post-transection (Fig. 7H, gray *vs.* white bars). In contrast, spinal cords treated with Syn MO exhibited nearly 2-fold more NF-180 labeled axons at all locations proximal and distal to the lesion, compared to untreated and MM MO-treated spinal cords (Fig. 7E–F, H; ANOVA $p < 2.0 \times 10^{-6}$). Thus, synuclein knockdown enhanced post-injury neuronal survival in the brain, as well as axon plasticity in the spinal cord.

4. Discussion

This is the first demonstration in any experimental model that synuclein accumulation plays a role in injury-induced neurodegeneration after SCI. Consequently, inhibiting post-injury synuclein accumulation with either an inhibitor of synuclein self-assembly, CLR01, or with a translation-blocking synuclein morpholino, significantly improved the survival of descending RS neurons. That CLR01 had a positive effect further suggests that the deleterious effects of synuclein can be corrected by attenuating its self-assembly into toxic oligomers. Furthermore, knocking down lamprey γ-synuclein accumulation increased the number of axons throughout the regenerated spinal cord. Thus, two independent strategies for reducing synuclein accumulation after SCI improved several anatomical measurements of recovery.

The simplest interpretation for the increased numbers of spinal axons after synuclein knockdown (Fig. 7) is that the increased number of surviving giant RS neurons in the brain led to a sparing of their axons in the spinal cord. However, there are indications of additional effects on axon sprouting and/or regeneration since the number of labeled axons after Syn MO treatment was even greater than that in the uninjured spinal cord. At present, the mechanisms leading to an increase in the number of spinal axons are unclear, but may include reduced or delayed axon retraction or Wallerian degeneration, increased regeneration or collateral sprouting from descending or ascending axons, or some combination, among other possibilities (Bradbury and McMahon, 2006; Blesch and Tuszynski, 2009).

The current findings were made possible by taking advantage of the features of lamprey giant RS neurons, where post-injury responses can be followed in individual, identified cells across a population of animals (Shifman et al., 2008; Busch and Morgan, 2012). However, it will now be important to investigate synuclein accumulation and its attenuation in other SCI models, including rodents, and the current literature suggests that our findings may apply to these other models. For example, increased α-synuclein immunoreactivity has been reported in motor neurons of rabbits after SCI (Sakurai et al., 2009). And, increased levels of α-, β- and γ-synuclein have been reported in cortical axons of mice and humans after TBI (Uryu et al., 2003; Uryu et al., 2007; Surgucheva et al., 2014). Furthermore, increased levels of α-synuclein have been observed in the brains and cerebral spinal fluid of TBI patients ranging from infants to adults (Uryu et al., 2007; Su et al., 2011; Mondello et al., 2013). Nonetheless, the fate of the neurons and the role of synuclein in injury-induced neurodegeneration have not been explored until now. We therefore predict that increased synuclein

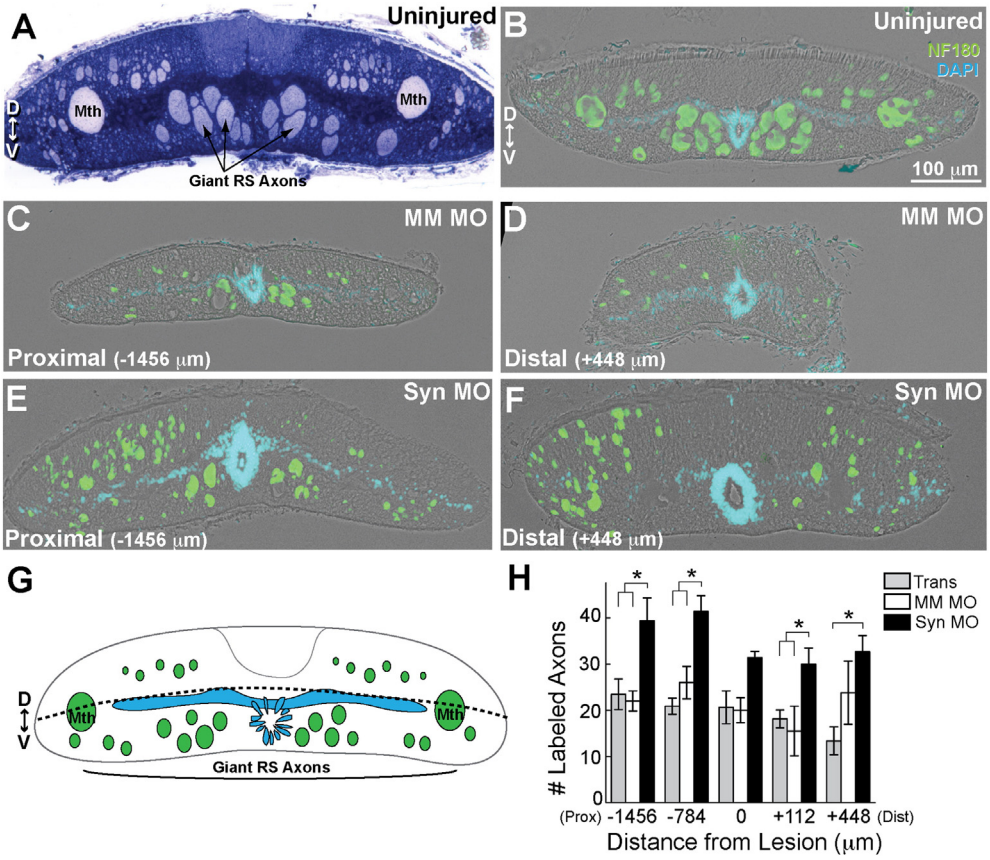

Fig. 7. Synuclein knockdown increases axon plasticity after SCI. A. Cross-section of an uninjured lamprey spinal cord stained with toluidine blue, showing the giant RS axons in the ventromedial tract, as well as the dorsolateral Mauthner (Mth) axon. Arrows indicate several RS axons. D = dorsal; V = ventral. B. Cryosection of an uninjured lamprey spinal cord showing immunolabeling of the giant RS axons with an NF-180 antibody (green). DAPI (blue) stains nuclei of ependymal cells within the central canal and motor neurons in the gray matter. Scale bar in B applies to C–F. C–D. At 11 weeks post-transection, spinal cords of animals treated with the mismatch control morpholino (MM MO) exhibited a reduced number of labeled axons both proximal and distal to the lesion. Distances from the lesion center are indicated. E–F. However, after treatment with the synuclein morpholino (Syn MO), there were substantially greater numbers of labeled axons throughout the spinal cord. G. NF-180 labeled axons in the ventral half of the spinal cord were analyzed. H. Syn MO significantly increased the number of axons throughout the spinal cord, as compared to MM MO and untreated, transected (Trans) controls. Bars represent mean ± S.E.M. from n = 4–8 spinal cords (*$p < 0.05$ by ANOVA, Tukey's post hoc).

immunoreactivity observed after injury in mammals is also due, at least in part, to synuclein aggregation and clearance deficiency within the degenerating neurons. As such, post-injury synuclein accumulation and related neurotoxicity may also be contributing to the poor outcomes after TBI (Su et al., 2011; Mondello et al., 2013). We propose that reducing synuclein accumulation could provide a potential means for improving neuronal survival and axon plasticity after injury in mammals, which should be explored in greater detail. Indeed, a very recent study showed that knocking down α-synuclein in the motor cortex improved both motor and sensory function after SCI in rats, compared to controls (Wang et al., 2016).

Between the data presented here and in our previous study, the mechanisms underlying post-injury synuclein accumulation are beginning to emerge (Busch and Morgan, 2012). In our previous study, using *in situ* hybridization, we showed that SCI induced a decrease in mRNA levels for lamprey γ-synuclein within the giant RS neurons. γ-Synuclein downregulation occurred in both good and poor survivors, though it was more extreme in the poor survivor population (Busch and Morgan, 2012). At the same time, synuclein protein accumulated in the somata, as described here, suggesting that post-transcriptional mechanisms and/or defects in protein processing or clearance are involved (Busch and Morgan, 2012). Impaired clearance is also supported by the appearance of atypically large ubiquitin inclusions in the poor survivors along with the synuclein accumulations (Busch and Morgan, 2012), and by the effects of CLR01 shown in this study. However, post-injury synuclein accumulation is unlikely to reflect a general inhibition of axonal transport of synaptic vesicles, because other synaptic vesicle-associated proteins, including synaptotagmin (Fig. 2I–L) and SV2 (Busch and Morgan, 2012), do not accumulate in response injury. Rather, blockage of the cellular clearance mechanisms, including the proteasome and autophagy, which have been reported to occur in Parkinson's disease models due to accumulation of toxic α-synuclein oligomers, are likely at play (Giorgi et al., 2006; Ferrucci et al., 2008; Emmanouilidou et al., 2010; Ebrahimi-Fakhari et al., 2011; Prabhudesai et al., 2012).

The fact that a translation-blocking morpholino reduced post-injury synuclein accumulation further indicates that this process involves post-transcriptional mechanisms. The morpholino effects also implicate synuclein accumulation as a dynamic process involving newly-translated protein (Fig. 5). It is not entirely clear why the mismatch control morpholino (MM MO) caused a greater amount of post-injury synuclein accumulation in the "good survivors" than is normally observed (Fig. 5F; compare with Fig. 3G) (Busch and Morgan, 2012). However, this atypical result lends even more support for our main conclusion, which is that post-injury synuclein accumulation is deleterious to neuronal survival, because the greater synuclein accumulation observed in "good survivors" after MM MO treatment resulted in decreased survival of these neurons (Fig. 6F). And, under these conditions, knocking down synuclein accumulation also ameliorated the deleterious effects by improving neuronal survival (Fig. 6F).

The effects of CLR01, which prevents α-synuclein aggregation *in vitro* and *in vivo* and facilitates α-synuclein clearance *in vivo*, provide additional insight into the mechanism of post-injury synuclein accumulation (Sinha et al., 2011; Prabhudesai et al., 2012a; Acharya et al., 2014).

Under conditions where synuclein levels remain low and normal, as in the untreated, transected "good survivors" (Fig. 3G), the protein likely is monomeric because CLR01 had no appreciable effect (Fig. 3G). However, when synuclein levels increase, as in the injured "poor survivors", synuclein likely self-associates into toxic oligomers and/or aggregates that impair clearance mechanisms, including the ubiquitin–proteosome system and autophagy (Cookson and van der Brug, 2008; Surguchov, 2008). Our data suggest that CLR01 prevents the formation of the toxic oligomers/aggregates and releases the clearance blockage after SCI, thus reducing the post-injury synuclein accumulation, which is similar to previous observations in a zebrafish model of α-synuclein neurotoxicity due to its overexpression (Prabhudesai et al., 2012). Importantly, CLR01 does not affect synuclein expression, but rather facilitates its clearance by remodeling the aggregation process into non-toxic and non-amyloidogenic structures. In zebrafish, this effect was shown to be mediated primarily by the 26S ubiquitin–proteasome system (Prabhudesai et al., 2012). Thus, the compound addresses directly the clearance deficit caused by the injury. More work is needed to determine how similar the post-injury synuclein assemblies are to the synuclein aggregates observed in Parkinson's disease and other synucleinopathies, and this should be investigated further.

Taken together, our findings suggest that reagents designed to reduce post-injury synuclein accumulation should either reduce synuclein translation and/or enhance its clearance in order to be effective. We do not yet know the precise contribution of synuclein translation *versus* aggregation in the neurodegenerative process or whether they impinge on a common mechanism. Interestingly, the positive effects of both CLR01 and Syn MO were observed after several months, even though the treatments were only single-dose applications at the time and site of injury. Thus, an interesting prospect is that early interventions that prevent post-injury synuclein accumulation may have long-lasting effects on the repair of the nervous system. Moreover, in addition to α-, β- and γ-synuclein, other proteins associated with neurodegenerative diseases, such as tau, amyloid β-protein precursor (APP), and amyloid β-protein (Aβ 1–42), have been reported to be elevated after TBI in animal models and humans (Uryu et al., 2007; Johnson et al., 2010). We do not yet know whether these other proteins form cytosolic aggregates after SCI in lampreys and may be additional targets of CLR01. However, the observations in mammals make CLR01 a particularly õattractive therapeutic approach because it is a broad-spectrum modulator of protein self-assembly and has been shown to reduce the accumulation of Aβ and hyperphosphorylated tau in a mouse model of Alzheimer's disease (Attar et al., 2012), in addition to reducing effects on neurotoxicity associated with α-synuclein overexpression (Prabhudesai et al., 2012). Data presented in this study therefore extend the potential utility of CLR01 beyond the neurodegenerative diseases to include SCI and possibly TBI.

In summary, we have identified synuclein accumulation as a factor that contributes to injury-induced neurodegeneration in the lamprey model of SCI. Although the precise homology between lamprey γ-synuclein and human synuclein orthologs is not clear (Busch and Morgan, 2012), lamprey γ-synuclein and human α-synuclein are highly conserved and can phenocopy each other to produce synaptic defects when acutely overexpressed at synapses (Busch et al., 2014), indicating some possible overlap in function. As such, synuclein accumulation (α-, β-, and γ-) should be further explored in rodent models following clinically-relevant spinal injuries, such as contusions and compressions, and eventually investigated as a potential target for therapeutic intervention after SCI.

Competing interests

FGK, TS, and GB are co-authors and co-inventors of International Patent Application No. PCT/US2010/026419, US Patent No. 13/203,962, European Patent Application 10 708 075.6. JM, DB, and GB are co-authors and co-inventors of Pending US Patent No. 14/536,176.

Acknowledgments

This work was supported by research grants from the Morton Cure Paralysis Fund and the NIH (RO1 NS078165 to JRM), a Parkinson's Disease Foundation summer student fellowship (PDF-SFW-1214 to AJVB), University of California-Los Angeles Jim Easton Consortium for Alzheimer's Drug Discovery and Biomarker Development (GB), and Team Parkinson/Parkinson Alliance (GB). The authors would like to thank Michele Nsianya and the 2013 Brown-MBL NeuroPracticum Course students for the technical assistance with immunofluorescence experiments, and Paul Oliphint for the histological image of the lamprey spinal cord.

References

Acharya, S., Safaie, B.M., Wongkongkathep, P., Ivanova, M.I., Attar, A., Klarner, F.G., Schrader, T., Loo, J.A., Bitan, G., Lapidus, L.J., 2014. Molecular basis for preventing alpha-synuclein aggregation by a molecular tweezer. J. Biol. Chem. 289, 10727–10737.

Attar, A., Ripoli, C., Riccardi, E., Maiti, P., Li Puma, D.D., Liu, T., Hayes, J., Jones, M.R., Lichti-Kaiser, K., Yang, F., Gale, G.D., Tseng, C.H., Tan, M., Xie, C.W., Straudinger, J.L., Klarner, F.G., Schrader, T., Frautschy, S.A., Grassi, C., Bitan, G., 2012. Protection of primary neurons and mouse brain from Alzheimer's pathology by molecular tweezers. Brain 135, 3735–3748.

Barreiro-Iglesias, A., Shifman, M.I., 2012. Use of fluorochrome-labeled inhibitors of caspases to detect neuronal apoptosis in the whole-mounted lamprey brain after spinal cord injury. Enzym. Res. 2012, 835731.

Becker, C.G., Lieberoth, B.C., Morellini, F., Feldner, J., Becker, T., Schachner, M., 2004. L1.1 is involved in spinal cord regeneration in adult zebrafish. J. Neurosci. 24, 7837–7842.

Bendor, J.T., Logan, T.P., Edwards, R.H., 2013. The function of alpha-synuclein. Neuron 79, 1044–1066.

Beyer, K., Ariza, A., 2008. The therapeutical potential of alpha-synuclein antiaggregatory agents for dementia with Lewy bodies. Curr. Med. Chem. 15, 2748–2759.

Blesch, A., Tuszynski, M.H., 2009. Spinal cord injury: plasticity, regeneration and the challenge of translational drug development. Trends Neurosci. 32, 41–47.

Bloom, O.E., Morgan, J.R., 2011. Membrane trafficking events underlying axon repair, growth, and regeneration. Mol. Cell. Neurosci. 48, 339–348.

Bradbury, E.J., McMahon, S.B., 2006. Spinal cord repair strategies: why do they work? Nat. Neurosci. Rev. 7, 644–653.

Busch, D.J., Morgan, J.R., 2012. Synuclein accumulation is associated with cell-specific neuronal death after spinal cord injury. J. Comp. Neurol. 520, 1751–1771.

Busch, D.J., Oliphint, P.A., Walsh, R.B., Banks, S.M., Woods, W.S., George, J.M., Morgan, J.R., 2014. Acute increase of alpha-synuclein inhibits synaptic vesicle recycling evoked during intense stimulation. Mol. Biol. Cell 25, 3926–3941.

Chandra, S., Gallardo, G., Fernandez-Chacon, R., Schluter, O.M., Sudhof, T.C., 2005. Alpha-synuclein cooperates with CSPalpha in preventing neurodegeneration. Cell 123, 383–396.

Cookson, M.R., 2009. alpha-Synuclein and neuronal cell death. Mol. Neurodegener. 4, 9.

Cookson, M.R., van der Brug, M., 2008. Cell systems and the toxic mechanism(s) of alpha-synuclein. Exp. Neurol. 209, 5–11.

Dawson, T.M., Ko, H.S., Dawson, V.L., 2010. Genetic animal models of Parkinson's disease. Neuron 66, 646–661.

Ebrahimi-Fakhari, D., Cantuti-Castelvetri, I., Fan, Z., Rockenstein, E., Masliah, E., Hyman, B.T., McLean, P.J., Unni, V.K., 2011. Distinct roles in vivo for the ubiquitin–proteasome system and the autophagy–lysosomal pathway in the degradation of alpha-synuclein. J. Neurosci. 31, 14508–14520.

Emmanouilidou, E., Stefanis, L., Vekrellis, K., 2010. Cell-produced α-synuclein oligomers are targeted to, and impair, the 26S proteasome. Neurobiol. Aging 31, 953–968.

Ferrucci, M., Pasquali, L., Ruggieri, S., Paparelli, A., Fornai, F., 2008. α-Synuclein and autophagy as common steps in neurodegeneration. Parkinsonism Relat. Disord. 14 (Suppl. 2), S180–S184.

Fujita, M., Sugama, S., Sekiyama, K., Sekigawa, A., Tsuki, T., Nakai, M., Waragai, M., Takenouchi, T., Takamatsu, Y., Wei, J., Rockenstein, E., LaSpada, A.R., Masliah, E., Inoue, S., Hashimoto, M., 2010. A β-synuclein mutation linked to dementia produces neurodegeneration when expressed in mouse brain. Nat. Commun. 1, 110.

Galvin, J.E., Uryu, K., Lee, V.M., Trojanowski, J.Q., 1999. Axon pathology in Parkinson's disease and Lewy body dementia hippocampus contains alpha-, beta-, and gamma-synuclein. Proc. Natl. Acad. Sci. 96, 13450–13455.

Giorgi, F.S., Bandettini di Poggio, A., Battaglia, G., Pellegrini, A., Murri, L., Ruggieri, S., Paparelli, A., Fornai, F., 2006. A short overview on the role of α-synuclein and proteasome in experimental models of Parkinson's disease. J. Neural Transm. Suppl. 105–109.

Hains, B.C., Black, J.A., Waxman, S.G., 2003. Primary cortical motor neurons undergo apoptosis after axotomizing spinal cord injury. J. Comp. Neurol. 462, 328–341.

Hu, J., Zhang, G., Selzer, M.E., 2013. Activated caspase detection in living tissue combined with subsequent retrograde labeling, immunohistochemistry or in situ hybridization in whole-mounted lamprey brains. J. Neurosci. Methods 220, 92–98.

Jacobs, A.J., Swain, G.P., Snedeker, J.A., Pijak, D.S., Gladstone, L.J., Selzer, M.E., 1997. Recovery of neurofilament expression selectively in regenerating reticulospinal neurons. J. Neurosci. 17, 5206–5220.

Jin, L.Q., Zhang, G., Jamison Jr., C., Takano, H., Haydon, P.G., Selzer, M.E., 2009. Axon regeneration in the absence of growth cones: acceleration by cyclic AMP. J. Comp. Neurol. 515, 295–312.

Johnson, V.E., Stewart, W., Smith, D.H., 2010. Traumatic brain injury and amyloid-beta pathology: a link to Alzheimer's disease? Nat. Rev. Neurosci. 11, 361–370.
Lau, B.Y., Fogerson, S.M., Walsh, R.B., Morgan, J.R., 2013. Cyclic AMP promotes axon regeneration, lesion repair and neuronal survival in lampreys after spinal cord injury. Exp. Neurol. 250, 31–42.
Lee, V.M., Trojanowski, J.Q., 2006. Mechanisms of Parkinson's disease linked to pathological alpha-synuclein: new targets for drug discovery. Neuron 52, 33–38.
Lulla, A., Barnhill, L., Bitan, G., Ivanova, M.I., Nguyen, B., O'Donnell, K., Stahl, M., Yamashiro, C., Klärner, F.-G., Schrader, T., Sagasti, A., Bronstein, J.M., 2016. Neurotoxicity of the Parkinson's disease-associated pesticide Ziram is synuclein dependent. (submitted for publication).
Mondello, S., Buki, A., Italiano, D., Jeromin, A., 2013. alpha-Synuclein in CSF of patients with severe traumatic brain injury. Neurology 80, 1662–1668.
Nemani, V.M., Lu, W., Berge, V., Nakamura, K., Onoa, B., Lee, M.K., Chaudhry, F.A., Nicoll, R.A., Edwards, R.H., 2010. Increased expression of alpha-synuclein reduces neurotransmitter release by inhibiting synaptic vesicle reclustering after endocytosis. Neuron 65, 66–79.
Ninkina, N., Peters, O., Millership, S., Salem, H., Putten, H.v.d., Buchman, V.L., 2009. g-Synucleinopathy: neurodegeneration associated with overexpression of the mouse protein. Hum. Mol. Genet. 18, 1779–1794.
Oliphint, P.A., Alieva, N., Foldes, A.E., Tytell, E.D., Lau, B.Y., Pariseau, J.S., Cohen, A.H., Morgan, J.R., 2010. Regenerated synapses in lamprey spinal cord are sparse and small even after functional recovery from injury. J. Comp. Neurol. 518, 2854–2872.
Prabhudesai, S., Sinha, S., Attar, A., Kotagiri, A., Fitzmaurice, A.G., Lakshmanan, R., Ivanova, M.I., Loo, J.A., Klärner, F.G., Schrader, T., Stahl, M., Bitan, G., Bronstein, J.M., 2012. A novel "molecular tweezer" inhibitor of α-synuclein neurotoxicity in vitro and in vivo. Neurotherapeutics 9, 464–476.
Rovainen, C.M., 1967. Physiological and anatomical studies on large neurons of central nervous system of the sea lamprey (*Petromyzon marinus*). I. Muller and Mauthner cells. J. Neurophysiol. 30, 1000–1023.
Roychaudhuri, R., Lomakin, A., Bernstein, S., Zheng, X., Condron, M.M., Benedek, G.B., Bowers, M., Teplow, D.B., 2014. Gly25-Ser26 amyloid beta-protein structural isomorphs produce distinct Abeta42 conformational dynamics and assembly characteristics. J. Mol. Biol. 426, 2422–2441.
Sakurai, M., Kawamura, T., Nishimura, H., Suzuki, H., Tezuka, F., Abe, K., 2009. Induction of Parkinson disease-related proteins in motor neurons after transient spinal cord ischemia in rabbits. J. Cereb. Blood Flow Metab. 29, 752–758.
Shifman, M.I., Zhang, G., Selzer, M.E., 2008. Delayed death of identified reticulospinal neurons after spinal cord injury in lampreys. J. Comp. Neurol. 510, 269–282.
Sinha, S., Lopes, D.H., Du, Z., Pang, E.S., Shanmugam, A., Lomakin, A., Talbiersky, P., Tennstaedt, A., McDaniel, K., Bakshi, R., Kuo, P.Y., Ehrmann, M., Benedek, G.B., Loo, J.A., Klarner, F.G., Schrader, T., Wang, C., Bitan, G., 2011. Lysine-specific molecular tweezers are broad-spectrum inhibitors of assembly and toxicity of amyloid proteins. J. Am. Chem. Soc. 133, 16958–16969.
Su, E., Bell, M.J., Wisniewski, S.R., Adelson, P.D., Janesko-Feldman, K.L., Salonia, R., Clark, R.S., Kochanek, P.M., Kagan, V.E., Bayir, H., 2011. alpha-Synuclein levels are elevated in cerebrospinal fluid following traumatic brain injury in infants and children: the effect of therapeutic hypothermia. Dev. Neurosci. 32, 385–395.
Surgucheva, I., He, S., Rich, M.C., Sharma, R., Ninkina, N.N., Stahel, P.F., Surguchov, A., 2014. Role of synucleins in traumatic brain injury — an experimental in vitro and in vivo study in mice. Mol. Cell. Neurosci. 63, 114–123.
Surguchov, A., 2008. Molecular and cellular biology of synucleins. Int. Rev. Cell Mol. Biol. 270, 225–317.
Uryu, K., Giasson, B.I., Longhi, L., Martinez, D., Murray, I., Conte, V., Nakamura, M., Saatman, K., Talbot, K., Horiguchi, T., McIntosh, T., Lee, V.M., Trojanowski, J.Q., 2003. Age-dependent synuclein pathology following traumatic brain injury in mice. Exp. Neurol. 184, 214–224.
Uryu, K., Chen, X.H., Martinez, D., Browne, K.D., Johnson, V.E., Graham, D.I., Lee, V.M., Trojanowski, J.Q., Smith, D.H., 2007. Multiple proteins implicated in neurodegenerative diseases accumulate in axons after brain trauma in humans. Exp. Neurol. 208, 185–192.
Vargas, K.J., Makani, S., Davis, T., Westphal, C.H., Castillo, P.E., Chandra, S.S., 2014. Synucleins regulate the kinetics of synaptic vesicle endocytosis. J. Neurosci. 34, 9364–9376.
Viscomi, M.T., Molinari, M., 2014. Remote neurodegeneration: multiple actors for one play. Mol. Neurobiol.
Wang, L., Das, U., Scott, D.A., Tang, Y., McLean, P.J., Roy, S., 2014. alpha-Synuclein multimers cluster synaptic vesicles and attenuate recycling. Curr. Biol. 24, 2319–2326.
Wang, Y.C., Feng, G.Y., Xia, Q.J., Hu, Y., Xu, Y., Xiong, L.-L., Chen, Z.-W., Wang, H.P., Wang, T.H., Zhou, X., 2016. Knockdown of α-synuclein in cerebral cortex improves neural behavior associated with apoptotic inhibition and neurotrophin expression in spinal cord transected rats. Apoptosis., PMID: 2682297 [Epub ahead of print].
Williams, R.R., Venkatesh, I., Pearse, D.D., Udvadia, A.J., Bunge, M.B., 2015. MASH1/Ascl1a leads to GAP43 expression and axon regeneration in the adult CNS. PLoS ONE 10, e0118918.
Yin, H.S., Selzer, M.E., 1983. Axonal regeneration in lamprey spinal cord. J. Neurosci. 3, 1135–1144.
Zhang, G., Jin, L.Q., Hu, J., Rodemer, W., Selzer, M.E., 2015. Antisense morpholino oligonucleotides reduce neurofilament synthesis and inhibit axon regeneration in lamprey reticulospinal neurons. PLoS ONE 10, e0137670.